



Experimental & Theoretical Analysis of Composite (Polyester & Silicon-Carbide) Cantilever Beam

Yousif K. Yousif

Ministry of Higher Education and Scientific Research/ Research & Development Department

Email: yousifky@gmail.com

(Received 2 April 2012; accepted 24 July 2012)

Abstract

A cantilever beam is made from composite material which is consist of (matrix: polyester) and (particles: Silicon-Carbide) with different volume fraction of particles. A force is applied at the free end of beam with different values. The experimental maximum deflection of beam which occurs at the point of the applied load is recorded. The deflection and slope of beam are analyzed by using FEM modeling. MATLAB paltform is built to assemble the equations, vector and matrix of FEM and solving the unknown variables (deflection and slope) at each node. Also ANSYS platform is used to modeling beam in finite element and solve the problem. The numerical methods are used to compare the results with the theoretical and experimental data. A good agreement is observed between the above methods. The Increase in volume fraction of particles results in increasing the modulus of elasticity and decreasing the deflection of beam. An equation is suggested for modulus of elasticity as functions of volume fraction.

Keywords: *composite beam, FEM, polyester, Silicon-Carbide.*

1. Introduction

Structures composed of composite materials offer lower weight and higher strength and stiffness than those composed of most metallic materials. That, coupled with advances in the manufacturing of composite materials and structures, gave them an edge when compared with normal engineering materials and led to their extensive use under complex mechanical and environmental loading. These composite structures can be modeled as simply supported beam or clamped beams.

Presents numerical and experimental results of active compensation of thermal deformation of a composite beam using piezoelectric ceramic actuators Finite-element modeling and experimental results agree well and demonstrate that the proposed method can actively perform structural shape control in the presence of thermal distortion [1].

An exact relationship between the slope increment of the beam end and the maximum slip at the support is presented, which makes possible

an easy and accurate evaluation of the beam deflection increment. This relationship is alidated both by numerical and experimental results [2].

An efficient one dimensional finite element model has been presented for the static analysis of composite laminated beams, using the efficient layer wise zigzag theory. The present zigzag finite element results for natural frequencies, mode shapes of cantilever and clamped-clamped beams are compared with the two-dimensional finite element results obtained using ABAQUS to establish the accuracy of the zigzag theory FEM for dynamic response under these boundary conditions [3].

Investigated the effects of shear slip on the deformation of steel-concrete composite beams. The equivalent rigidity of composite beams considering three different loading types was first derived based on equilibrium and curvature compatibility, for full composite sections, the effective section modulus and moment of inertia calculated with the AISC specifications are larger than that of present study. For partial composite

sections, the AISC predictions are more conservative than the present study [4].

Investigate the structural behavior of concrete-encased composite beam–columns with T-shaped steel section. The test results indicate that the cyclic behavior and failure modes of the beam–columns are greatly affected by the direction of the bending moment owing to the unsymmetrical cross section. [5]

Reviews the available literature on the state of the art of prefabricated wood composite I-beams. The results of analytical and experimental investigations illustrate the effects of materials, Joint, geometry, and environment on the short- and long-term performance of I-beams.[6]

2. Experimental Work

2.1. Composite Material

The material used in this work is made from composite material including:

- Matrix: polyester.
- Particle: powder of Silicon-Carbide

A homogenous mixing of powder with the polyester is done with the following particles volume fraction:

Table 1, Volume Fraction of Silicon-Carbide Particles.

Vp %	0.1	0.2	0.3	0.4	0.5	0.6	0.7	0.8	0.9	1
------	-----	-----	-----	-----	-----	-----	-----	-----	-----	---

Each volume fraction gives new composite mechanical properties as comparing with the matrix or particle. The important property of composite material here is the modulus of elasticity (E). The value of (E) depends on volume fraction, modulus of elasticity for each matrix and particle material and given by the following equation [7]:

$$E = V_m E_m + V_p E_p \quad \dots (1)$$

Where:

E: modulus of elasticity of composite material (N/mm²)

V_m: matrix volume fraction

V_p: particle volume fraction

E_m: matrix modulus of elasticity (2000N/mm²)

E_p: particle modulus of elasticity (4*10⁵N/mm²)

To calculate the modulus of elasticity (E) for the composite material, sub the above value of (E_m,E_p) and the values of (V_m,V_p) from table (1)

in the above equation(1). The results values of (E) are given in Table (2).

Table 2, Modulus of Elasticity for Each Volume Fraction.

Vp %	E(N/mm ²)
0.1	2398
0.2	2796
0.3	3194
0.4	3592
0.5	3990
0.6	4388
0.7	4786
0.8	5184
0.9	5582
1	5980

2.2. Beam Preparation and Boundary Conditions

The sample of beam is made from composite material consist of (matrix: polyester) and (particle: Silicon Carbide). The beam sample is made with different volume fraction as mentioned. The geometry of beam is shown in Fig. (1) :

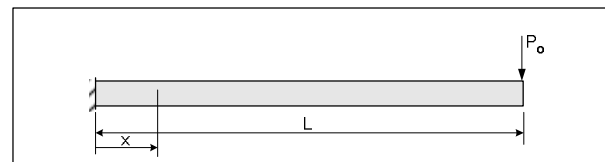


Fig. 1. Cantilever Beam with Free end Load.

*rectangular cross sectional area with:

Width: b= 13 mm.

Height: h= 6 mm.

*length: L= 191 mm.

A concentrated load is applied at the free end of beam length (x=L) to give a maximum deflection at this point. The state of boundary conditions for cantilever beam is given as follow:

Deflection & slope=0 at (x=0).

The values of forces used in this work are given in Table (3).

Table 3, The Values of Load Used.

P(N)	0.981	1.962	2.943	3.924	4.905	5.886
------	-------	-------	-------	-------	-------	-------

3. Theoretical Analysis

The deflection of concentrated force beam (Fig.(1)) given in the following equation[8]:

$$y = d = \frac{Px^3}{6EI} - \frac{Px^2L}{2EI} \quad \dots(2)$$

Hence, the maximum deflection occurred at the free end(x=L):

$$d = \frac{PL^3}{3EI} \quad \dots(3)$$

Differentiate Eq.(2) to give the slope of beam ($\theta=dy/dx$):

$$dy/dx = \theta = \frac{Px^2}{2EI} - \frac{PxL}{EI} \quad \dots(4)$$

Where:

I: moment of inertia. Its equation in this work is:

$$I = \frac{bh^3}{12} \quad \dots(5)$$

The beam dimensions (b=13 mm; h=6 mm), therefore, the value of I is:

$$I = 234\text{mm}^4.$$

4. Finite Element Method

The analysis of finite element equations is based on the Euler-Bernoulli equation for beam bending [9, 10, and 11]:

$$r \frac{\partial^2 v}{\partial t^2} + \frac{\partial^2}{\partial x^2} (EI \frac{\partial^2 v}{\partial x^2}) = q(x, t) \quad \dots(6)$$

where:

$v(x,t)$: transverse displacement of the beam.

ρ : mass density per volume.

EI: beam rigidity.

$q(x,t)$: external applied pressure loading.

t,x :time and spatial axis along the beam axis.

Applying one of the methods of weighted residual, Galerkin's method, to the beam equation (Eq.(6)) to develop the finite element formulation and the corresponding matrix equations.

The weight residual of Eq.(6) is :

$$\int_0^l (r \frac{\partial^2 v}{\partial t^2} + \frac{\partial^2}{\partial x^2} (EI \frac{\partial^2 v}{\partial x^2}) - q) w dx = 0 \quad \dots(7)$$

where:

L: length of beam.

w: a test function.

Describe the beam in to a number of finite element, integrate Eq.(7) by parts twice for the second term gives:

$$\Pi = \sum_{i=1}^n \int_{\Omega^e} \rho \frac{\partial^2 v}{\partial t^2} w dx + \int_{\Omega^e} EI \frac{\partial^2 v}{\partial x^2} \frac{\partial^2 w}{\partial x^2} dx - \int_{\Omega^e} q w dx + [V_m - M \frac{\partial w}{\partial x}]_0^l = 0 \quad \dots(8)$$

Where:

$$V_m = EI \frac{\partial^3 v}{\partial x^3} : \text{shear force.}$$

$$M = EI \frac{\partial^2 v}{\partial x^2} : \text{bending moment.}$$

Ω^e :an element domain.

n :number of elements for beam.

The shape function is considered in term of nodal variable. Assume beam element have two nodes one at each end as shown in Fig. (2).

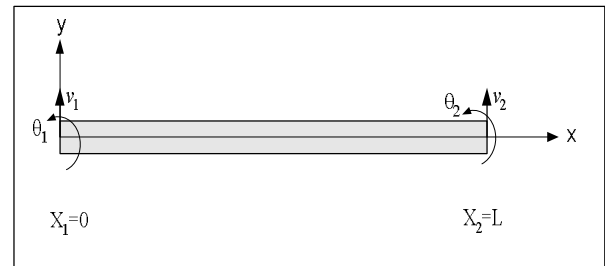


Fig. 2. Deflection and Slope of Each Node in Element.

The deformation of beam must have continuous slope as well as continuous deflection at any neighboring beam elements (slope: θ_i , deflection: v_i), as nodal variables. The Euler-Bernoulli equation for beam bending is based on the assumption that the plane normal to the neutral axis before deformation remains normal to the neutral axis after deformation. The deflection equation is assumed as a cubic polynomial:

$$v(x) = c_0 + c_1 x + c_2 x^2 + c_3 x^3 \quad \dots(9)$$

The slope can be found by differentiate eq.(9) w.r.t. x as follow:

$$q(x) = c_1 + 2c_2 x + 3c_3 x^2 \quad \dots(10)$$

The deflection and slope at each node yield:

$$\begin{aligned}
 v(0) &= c_0 = v_1 \\
 q(0) &= c_1 = q_1 \\
 v(l) &= c_0 + c_1l + c_2l^2 + c_3l^3 = v \quad \dots(11) \\
 q(l) &= c_1 + 2c_2l + 3c_3l^2 = q_2
 \end{aligned}$$

Solving eq.(11) for ci in term of nodal variable (deflection and slope) and substituting the results into eq.(9) gives:

$$\begin{aligned}
 v(x) &= H_1(x)v_1 + H_2(x)q_1 + H_3(x)v_2 \\
 &+ H_4(x)q_2 \quad \dots(12)
 \end{aligned}$$

Where:

$$\begin{aligned}
 H_1(x) &= 1 - \frac{3x^2}{l^2} + \frac{2x^3}{l^3} \\
 H_2(x) &= x - \frac{2x^2}{l} + \frac{x^3}{l^2} \\
 H_3(x) &= \frac{3x^2}{l^2} - \frac{2x^3}{l^3} \\
 H_4(x) &= -\frac{x^2}{l} + \frac{x^3}{l^2}
 \end{aligned} \quad \dots(13)$$

The function Hi are called Hermitian shape function. Application of this function and Galerkin’s method to the second term of eq.(8) results in the stiffness matrix of the beam element. That is :

$$[K^e] = \int_0^l [B]^T EI [B] dx \quad \dots(14)$$

Where:

$$[B] = \{ H''_1, H''_2, H''_3, H''_4 \} \quad \dots(15)$$

The corresponding element nodal degrees of freedom are:

$$\{d^e\} = \{v_1 \ q_1 \ v_2 \ q_2\} \quad \dots(16)$$

Differentiate the shape function twice and sub the results in eq.(15) which can be sub in eq.(14) to find the integration results of the element stiffness matrix as follows:

$$[K^e] = \frac{EI}{l^3} \begin{bmatrix} 12 & 6l & -12 & 6l \\ 6l & 4l^2 & -6l & 2l^2 \\ -12 & -6l & 12 & -6l \\ 6l & 2l^2 & -6l & 4l^2 \end{bmatrix} \quad \dots(17)$$

The third term of eq.(8) represented as a concentrated load in this work, Fig. (3), the element force vector is :

$$\{F^e\} = \int_0^l p_o d(x-x_o) \begin{Bmatrix} H_1 \\ H_2 \\ H_3 \\ H_4 \end{Bmatrix} dx = p_o \begin{Bmatrix} H_1(x_o) \\ H_2(x_o) \\ H_3(x_o) \\ H_4(x_o) \end{Bmatrix} \quad \dots(18)$$

where:

Po: the concentrated load applied at x=xo.
 δ(x=xo) : dirac diltla function.

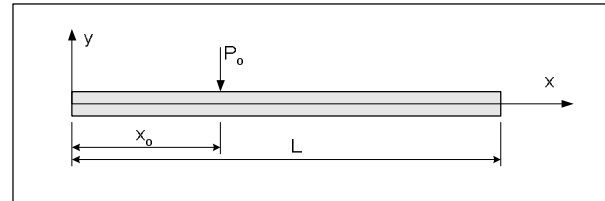


Fig. 3. The Location of Concentrated Load in Element.

For the static bending analysis of beams, the first term of eq.(8) which is the inertia force is neglected. The last term in the same above equation is the boundary conditions of shear and bending moment at the two points (x=0 & x=L). Only a concentrated force is used at the free end of beam, therefore, the last term of eq.(8) will neglect.

Assembling the element stiffness matrices and vector results in the system matrix equation given below:

$$[K]\{d\} = \{F\} \quad \dots(19)$$

4.1. Finite Element Programming

The finite element method [12] has been done using a MATLAB platform. The steps of this platform are shown in Fig. (4) and explained as follows:

Step (1): in this step, it assumed that the number of element used is five with (6 nodes). Each node has two degree of freedom.

Step (2): material properties represented by input the modulus of elasticity for each value of volume fraction which is described in Table (2) of the experimental work.

Input the beam dimensions included the width, height and its length.

Step (3): in finite element analyzing, it assume a half beam due to symmetry; therefore the boundary conditions will be:

At the fixd end (x=0, deflection=0, slope=0).

Step (4):the applied load will concentrate at the free end of beam and its value be (F).

Step (5): element stiffness can be evaluated from eq.(17).

Step (6): global element stiffness has been evaluated for the half beam as matrix of dimension (12*12).

Step (7): solve eq.(19) to give the deflection and slope at each node.

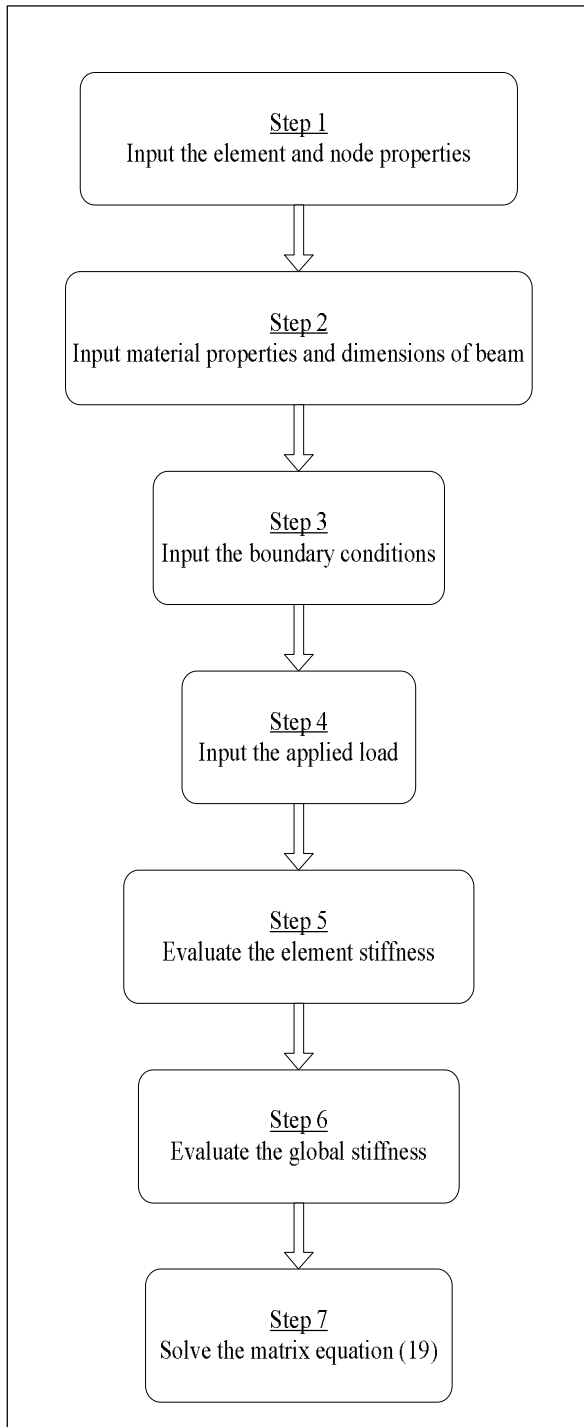


Fig. 4. Steps of Finite Element Method.

5. Beam Modeling in ANSYS Platform

ANSYS 11 platform is used to analyze the deflection and slope of beam which is defined by ten elements (11 nodes) as shown in Fig. (5). The material property (E), beam dimensions (b,h,L) and boundary conditions is given as input data from the experimental work. Also the concentrated load is applied at the free end of beam length (node 11: $x=L$).

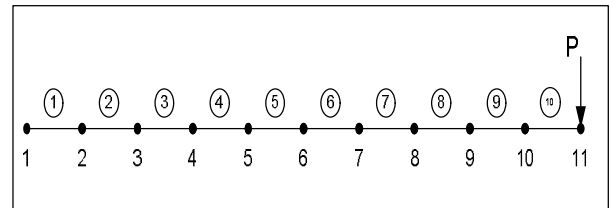


Fig. 5. Element and Node Numbering of Beam in ANSYS Platform.

6. The Result

The experimental results are plotted in figures (6-15) for wide range of concentrated force. Each figure represent the variation of maximum beam deflection (at $x=L$) with the applied concentrated load at the same point for each volume fraction mentioned in the experimental work. Theoretical, finite element method and the analyzing of beam deflection using ANSYS paltform are used here to compare the result data of those methods with the experimental data. Basically, increasing the concentrated load results in increasing the deflection of beam. The models of FEM and ANSYS platform for analysis the deflection of beam gives a good agreement with the theoretical analysis as well as with the experimental data. In general, the relation between the applied load and the deflection has a linear function. As it has been observed, the experimental data are alternate about the theoretical, FEM and ANSYS results with small error. A scatter experimental data are observed which may be due to the mistake recording of equipment.

Variation of maximum deflection with volume fraction for each load is shown in Figure (16). Increasing the volume fraction of Silicon-Carbide particles results in decreasing the deflection with a smooth curve . This is due to increasing the modulus of elasticity of composite material with increasing the volume fraction of particles as in Table (2).

FEM and ANSYS platform gives the deflection for each point of beam as well as the slope of beam at each point. A sample results is choose for the applied load (P=5.886 N) and volume fraction (Vp=0.1%) shown in Figure (17). A good agreement is observed as comparing the numerical method with the theoretical equation.

The deformed shape resulted from the ANSYS platform for the same above force and volume fraction is shown in figures (18 & 19) for deflection and slope results respectively.

On the other hand another suggested equation can be found for the modulus of elasticity for composite material of this work as a function of volume fraction of particle. Figure (20) show the graph of modulus of elasticity with particle volume fraction. The linear equation can be represented as follow:

$$E(Vp) = 2000 + 398000 * Vp \quad \dots (20)$$

Where (Em=2000 GPa), the above equation can be written in another form as follow:

$$E(Vp)=Em+398000*Vp \quad \dots(21)$$

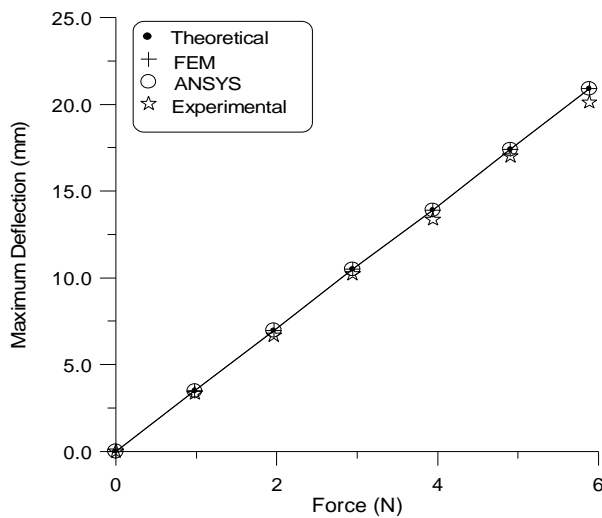


Fig. 6. Variation of Deflection with the Applied Force (Vp=0.2%).

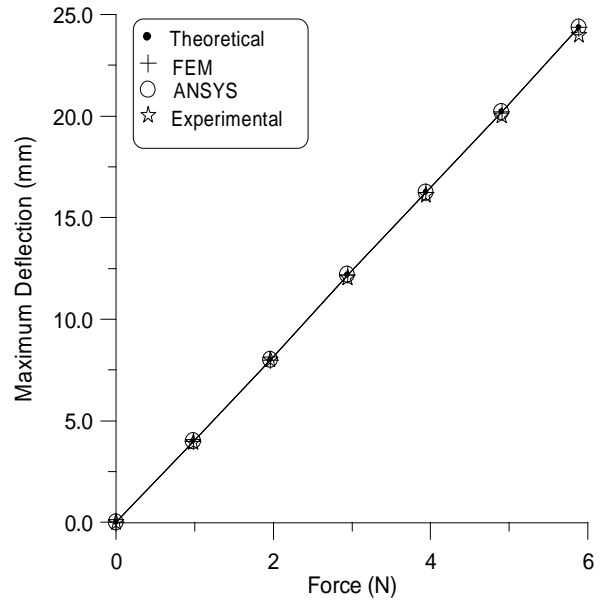


Fig. 7. Variation of Deflection with the Applied Force (Vp=0.1%).

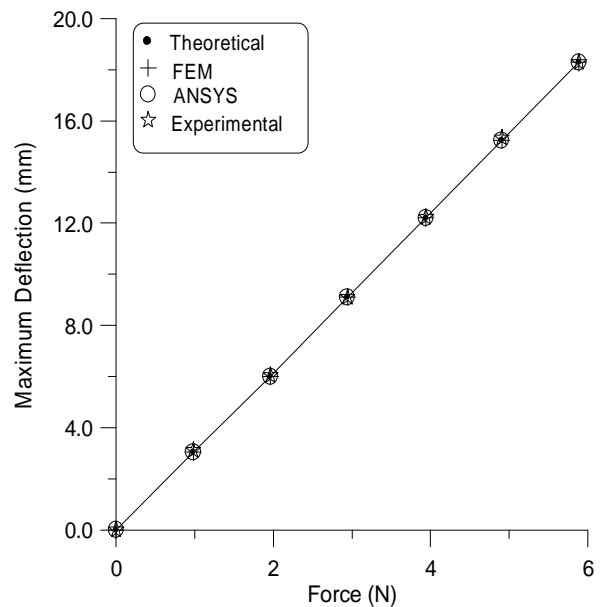


Fig. 8. Variation of Deflection with the Applied Force (Vp=0.3%).

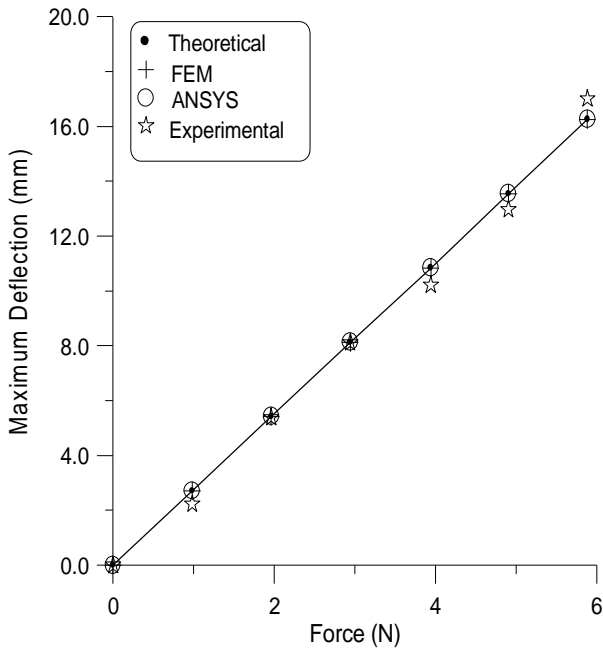


Fig. 9. Variation of Deflection with the Applied Force (Vp=0.4%).

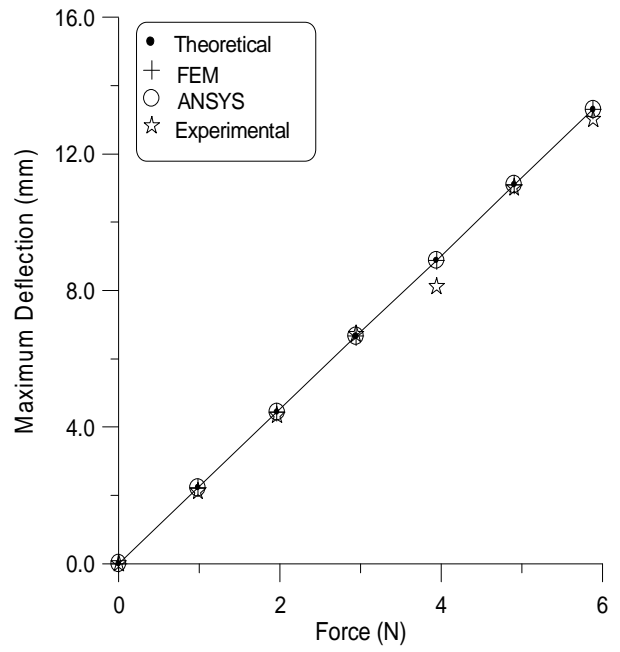


Fig. 11. Variation of Deflection with the Applied Force (Vp=0.6%).

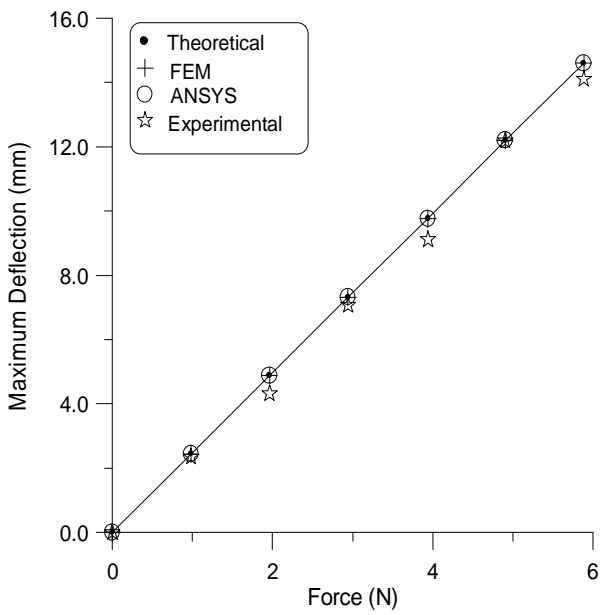


Fig. 10. Variation of Deflection with the Applied Force (Vp=0.5%).

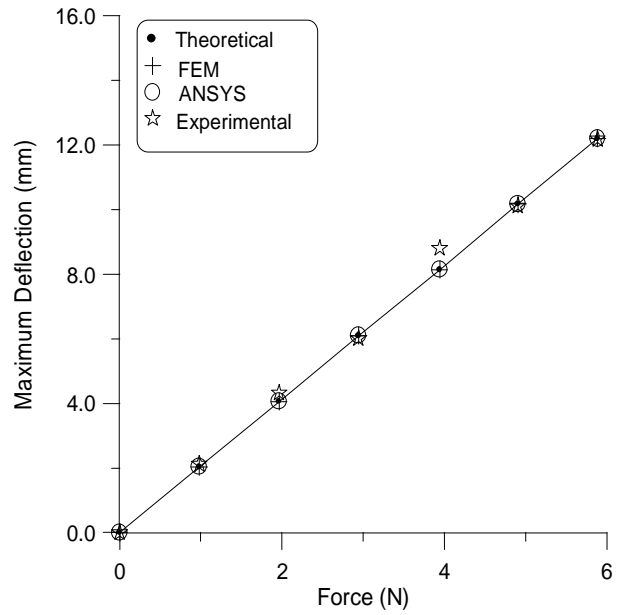


Fig. 12. Variation of Deflection with the Applied Force (Vp=0.7%).

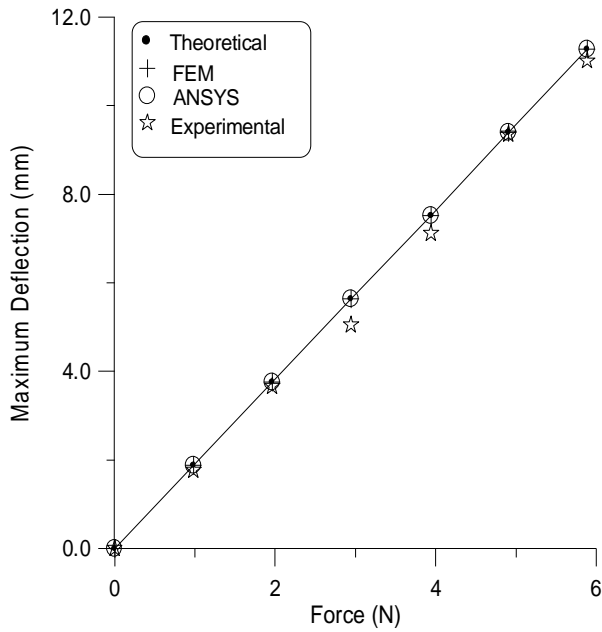


Fig. 13. Variation of Deflection with the Applied Force ($V_p=0.8\%$).

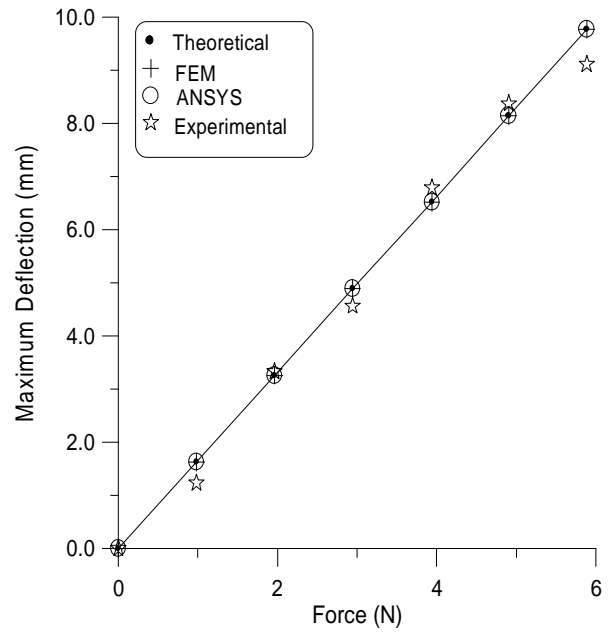


Fig. 15. Variation of Deflection with the Applied Force ($V_p=1\%$).

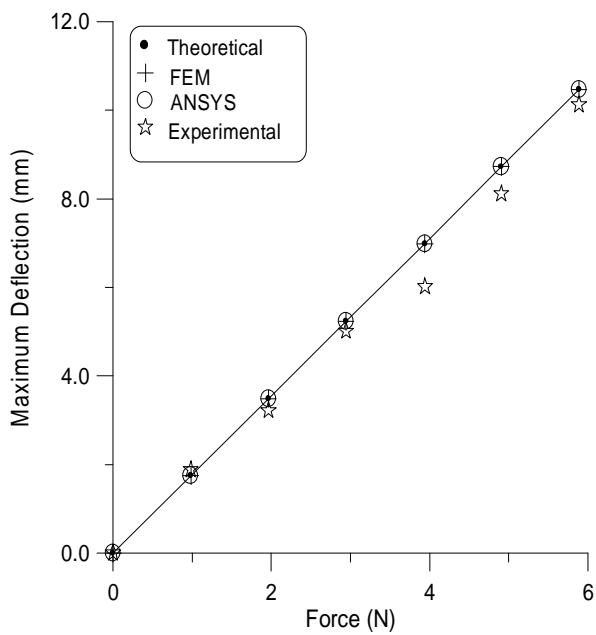


Fig. 14. Variation of Deflection with the Applied Force ($V_p=0.9\%$).

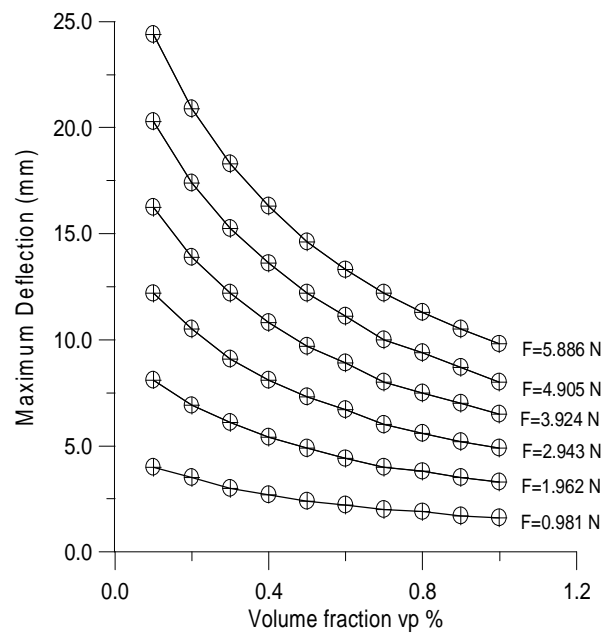


Fig. 16. Variation of Deflection with the Volume Fraction .

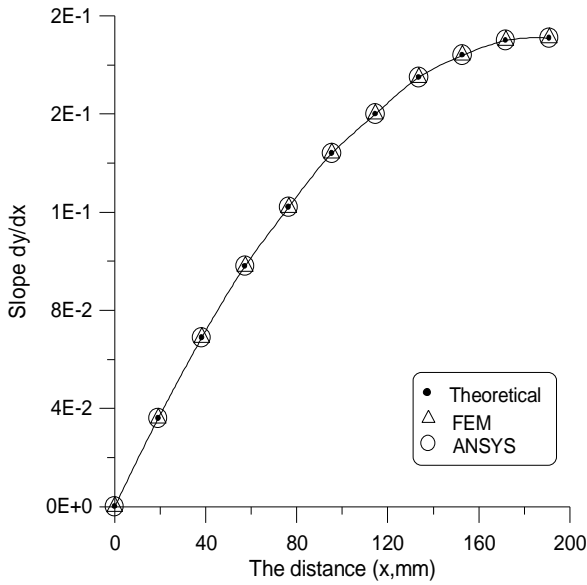


Fig. 17. Variation of Slope with the Distance (x).

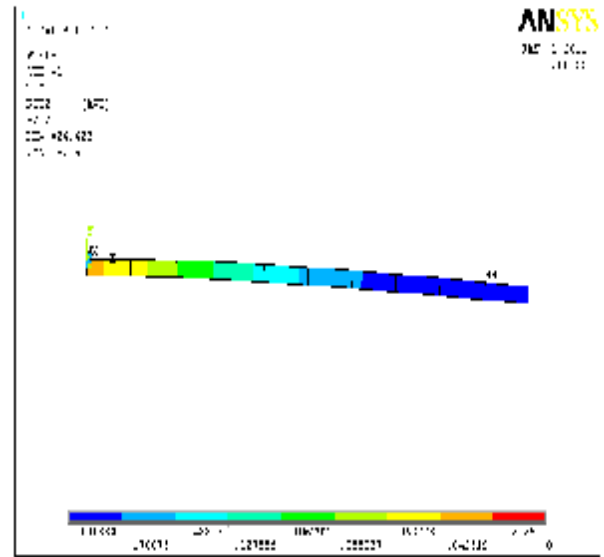


Fig. 19. Variation of Slope Along Beam Length for (P=5.886 N) and (Vp=0.1%), ANSYS Platform.

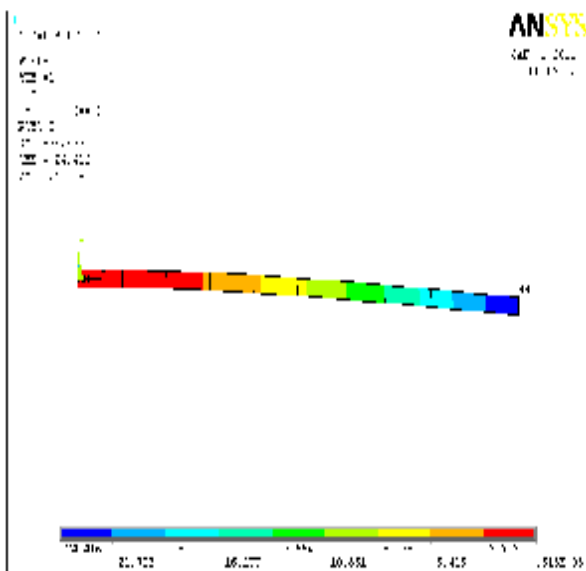


Fig. 18. Variation of Deflection along Beam Length for (P=5.886 N) and (Vp=0.1%), ANSYS Platform.

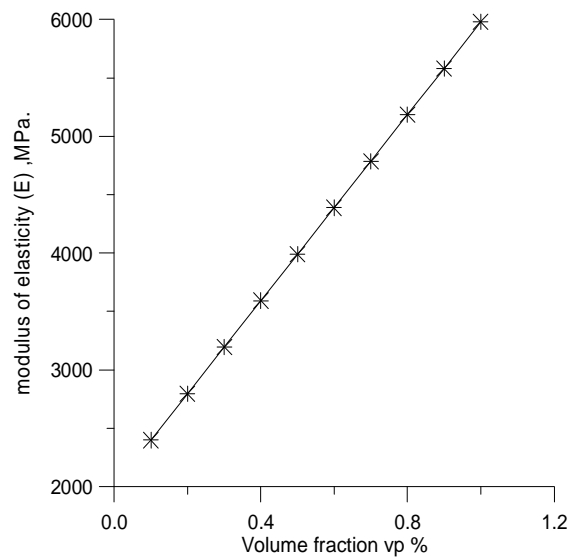


Fig. 20. Variation of (E) with Volume Fraction.

7. Conclusions

The theoretical FEM analysis for the deflection of beam gives a good agreement with the experimental results.

Experimental

Increasing the volume fraction of Silicon-Carbide particles, decreasing the deflection of beam for the same applied force & increasing the modulus of elasticity of composite material with increasing the volume fraction of particles.

Theoretical

The slope calculated from the FEM and ANSYS program gives a good agreement comparing with the theoretical equation.

The relation between the deflection reduction and the volume fraction is suggested as a polynomial third order equation.

A linear equation for the modulus of elasticity for the composite material as a function of volume fraction and matrix modulus of elasticity is observed and the fitting of this equation is suggested.

8. References

- [1] G. Song¹, X. Zhou and W. Binienda "Thermal deformation compensation of a composite beam using piezoelectric actuators" SMART materials and structure, institute of physics publishing, Smart Mater. Struct. 13 (2004) 30–37 .
- [2] P. Gelfi and E. Giuriani "Influence of Slab-Beam Slip on the Deflection of Composite Beams" International Journal for Restoration of Buildings and Monuments Vol. 9, No 5, 475–490 (2003)
- [3] M. Naushad Alam and Nirbhay Kr. Upadhyay "Finite Element Analysis of Laminated Composite Beams for Zigzag Theory using MATLAB" International Journal of Mechanics and Solids , ISSN 0973-1881 Volume 5, Number 1 (2010), pp. 1-14
- [4] Jianguo Nie¹ and C. S. Cai, P.E., M.ASCE "Steel–Concrete Composite Beams Considering Shear Slip Effects", journal of structures engineering ASCE / April 2003.
- [5] Cheng-Chih Chen, Jian-Ming Li, C.C. Weng , "Experimental behavior and strength of concrete-encased composite beam–columns with T-shaped steel section under cyclic loading", Journal of Constructional Steel Research 61 (2005) 863–881.
- [6] Robert J. Leichti , Robert H. Falk and Theodore L. Laufenberg "prefabricated wood composite I-beams: a literature review " Wood and Fiber Science, 2(1), 1990, pp. 62-79.
- [7] Autar K. Kaw " mechanics of composite materials" Taylor & Francis Group, LLC,2006.
- [8] Lloyd Hmlton Donnell "Beams, Plates and Shells" McGraw-Hill, Inc. 1976.
- [9] O.C. Zienkiewics, Frs. "the finite element method" Mc. Graw Hill Book Company (UK) limited 1977.
- [10] Tirupathir. Chandrupathla and Ashok D.Belegundu "finite element in engineering" Prentice/hall of India,1977.
- [11] James Doyle "Finite element methods" John Wiley & Sons, Ltd 2004.
- [12] Hinton and D.R.J. Owen. " Finite element Programing" Academic Press Inc. (London) LTD.1983.

التحليل النظري والعملي للمادة المركبة (البوليستر ودقائق كاربيد- السيلكون) لعتبة مثبتة

يوسف خلف يوسف

وزارة التعليم العالي والبحث العلمي / دائرة البحث والتطوير
البريد الإلكتروني: yousifky@gmail.com

الخلاصة

تم تصنيع عتبة مثبتة من طرف وحررة من طرف اخر من المادة المركبة (البوليستر ودقائق كاربيد- السيلكون) بقيم مختلفة من الكسر الحجمي. ان القوى المسلطة عند النهاية الحرة للعتبة. قيم أقصى انحراف للعتبة و قرأت مختبريا عند نقطة تسليط القوة. انحراف وميلان العتبة تم تحليله باستخدام طريقة العناصر المحددة. حيث تم تجميع معادلات، متجهات ومصفوفة هذه الطريقة باستخدام برنامج MATLAB وحل المتغيرات المجهولة (الانحراف والميلان) عند كل عقدة. أيضا تم استخدام برنامج أل (ANSYS) لتحليل العتبة بطريقة العناصر المحددة. الطرق العددية استخدمت لمقارنة النتائج مع النتائج النظرية والعملية. تمت ملاحظة توافق جيد بين تلك النتائج النظرية والعملية. ان زيادة الكسر الحجمي للحبيبات أدى إلى زيادة معامل المرونة ونقصان انحراف العتبة.